

# Numerical Investigation on Thermal Performance of Plate-Fin Heat Sink Designs Subjected to Parallel and Impinging Flow

Muhammad Zarif Bin Shaharudin<sup>1</sup>, Syahar Shawal<sup>1,\*</sup>, M. Mazwan Mahat<sup>1</sup>, Juri Saedon<sup>1</sup>, MS Meon<sup>1</sup>, and Mohd Rosdzimin Abdul Rahman<sup>2</sup>

<sup>1</sup>School of Mechanical Engineering, College of Engineering, Universiti Teknologi MARA, 40450 Shah Alam, Selangor, Malaysia.

<sup>2</sup>Department of Mechanical Engineering, Faculty of Engineering, Universiti Pertahanan Nasional Malaysia, Kem Sg. Besi, 57000, Kuala Lumpur, Malaysia.

\*corresponding author: syahar6595@uitm.edu.my

## ABSTRACT

The electronic industry has been working for decades to improve the cooling efficiency of heat sinks by creating more advanced, efficient cooling technologies. However, heat dissipation remains the major problem due to the designs complexity and limited space for cooling devices. This paper investigates the effect of flow direction on the thermal performance for the proposed designs. The removed material from the fin base to create the fillet was re-used to form half-round pin that was attached to the plate-fin, in symmetrical and corrugated arrangements. Plate-fin heat sinks with and without fillet profiles were investigated and two new proposed designs for plate-fin heat sinks with half-round pins attached to the fin were developed in this study. Numerical analysis was performed using ANSYS FLUENT R21 to evaluate the thermal performance of the proposed designs. For the element optimization, the grid independency test was performed to obtain the optimal number of elements. A constant heat flux of 18.75 kW/m<sup>2</sup> was applied at the bottom plate of heat sinks as the input parameter and two different flow directions e.g., impinging flow and parallel flow at various mass flow rate was also applied to study the base temperature, thermal resistance and Nusselt number of these designs. The study has shown that plate-fin heat sinks with fillet profile and corrugated half-round pins (PFHS 4) subjected to parallel flow and plate-fin heat sinks with fillet profile and symmetrical half-round pins (PFHS 3) subject to impinging flow exhibit better thermal performance over other configurations. Hence, these plate-fin designs have the potential to be practically applied as heat sinks for electronic devices.

**Keywords:** Plate-fin heat sinks, thermal performance, numerical method

## Nomenclature

$A_T$	heat sink surface area (m <sup>2</sup> )
$h$	average convective heat transfer coefficient (W/m <sup>2</sup> . °C)
$Nu$	average Nusselt number (-)
$Q$	heat transfer rate (W)
$R_{th}$	thermal resistance (°C /W)
$T_m$	average air temperature (°C)

## Abbreviations

PFHS 1	Plate-fin heat sinks without fillet profile
PFHS 2	Plate-fin heat sinks with fillet profile
PFHS 3	Plate-fin heat sinks with fillet profile and symmetrical half-round pins
PFHS 4	Plate-fin heat sinks with fillet profile and corrugated half-round pins

## 1.0 INTRODUCTION

Due to recent advancements in semiconductor technology, power density in electronic and microelectronic equipment is increasing rapidly. The miniaturization of electronic devices has posed a difficulty for thermal management of such devices since overheating can lead to reduction in device performance. As a result, in a strong competitive electronic device business, increasing the heat transfer rate of electronic devices is crucial for long-term reliability. A heat sink is a component that allows more heat to be transferred away from a hot device. It achieves this by expanding the device's operating surface area and the amount of low-temperature fluid that

flows through it [1]. Many industrial devices such as computer processors and air conditioning systems utilize heat sinks. Copper and aluminium are two typical metals used to manufacture heat sinks. To enhance the heat dissipation area, most heat sinks are built with fins that are attached to the heat sink base. Heat transfer improvement can be done in two ways, either active or passive [2,3].

Finned heat sinks are used in various engineering systems to dissipate excessive heat to the surrounding through convection mechanics. Heat sinks are equipped with peripherals like jets and fans to fulfil the demand for more heat dissipation [4]. The parallel arrangements of rectangular cross section plate fins or pin fins on a flat base are two of the most widely applied heat sink configurations. Plate-fin heat sinks are one type whereas pin-fin heat sinks are another.

Several studies have shown the comparison of the cooling efficiency of these configurations. F. Forghan et al. [5,6] found that for low air velocities, the thermal performance of pin-fin heat sinks is significantly lower than plate-fin heat sinks. However, research has shown that the thermal performance of a pin-fin heat sink is better to that of a plate-fin heat sink under certain situations [7,8]. Kim et al. [9] compared the thermal performance of plate-fin and pin-fin heat sinks subjected to impinging flow by performing experimental and analytical investigation. The pressure drop and thermal resistance of both configurations were predicted using a model based on the volume averaging approach. They discovered that when the heat sink's dimensionless length is high and the dimensionless pumping power is low, the optimized pin-fin heat sinks exhibit lower thermal resistance than the optimized plate heat sinks. Plate-fin heat sinks, on the other hand, have the least thermal resistance when the dimensionless pumping power is high and the dimensionless length of the heat sink is small.

A number of research has also focused on fully realizing the thermal performance enhancement that finned heat sinks offer by introducing new types of fin configurations which are not restricted to the typical types of heat sinks. For example, Hosseini et al. [10] investigated the effect of two types of splitter shape namely wavy splitter and arched splitter on the cooling efficiency of thermal-hydraulic plate-fin heat sinks in both forward and backward arrangements. They found that arched splitter in a forwarding arrangement provides the lowest base temperature that leads to a greater thermal performance. Other studies also included flared fins [5], oblique planar fins [11], rectangular perforation fins [12,13], square and circular perforation fins [14], square perforation fins [15-17], triangular perforations [18], radial heat sinks [19] and plate-fins with fillet profile [20]. Researchers also focused on the geometry of the heat sink's fin. As for plate-fin heat sinks, the effect of fin number and thickness on thermal performance have been investigated analytically in [21], and the influence of the height and width of fins have been studied both numerically and experimentally in [22][23].

Furthermore, due to the limited space for placing cooling fans in electronic devices, the effect of flow direction and configuration (i.e. impinging flow and parallel flow) on the enhancement of cooling efficiency of plate-fin heat sinks was also studied by various researchers. Biber [28] developed a numerical model to investigate the effect of impinging flow on pressure drop and cooling capacity of single isothermal channels. Correlations for pressure loss coefficient and average Nusselt number in a variable-length channel cover a wide range of practical plate-fin heat sinks. These correlations may then be used to predict the thermal performance of the heat sink. Saini and Webb [29] validated Biber model [28] by experiment data. Duan and Muzychka [30] developed a simple semi-empirical model for predicting the pressure drop and the heat transfer coefficient of air-cooled plate-fin heat sinks.

This paper intends to close this gap by evaluating the thermal performance of a new proposed design under both parallel and impinging flow conditions, while taking into account the level of complexity to fabricate the designs. The removed material from the fin base to create the fillet was re-used to form half-round pin that was attached to the plate-fin, in symmetrical and corrugated arrangements. Therefore, this study aims to investigate the effect of fillet profile on heat transfer characteristics and evaluates the thermal performance of different design plate-fin heat sinks subjected to parallel and impinging flow.

## 2.0 METHODOLOGY

### 2.1 Geometrical modelling

The model of the plate-fin heat sinks (PFHC) was created using CATIA V5 software. Then, the CAD model was transferred to the ANSYS FLUENT R21 for the simulation process. The parallel rectangular arrangement of fins on a flat base was used to model the plate-fin heat sinks. Figure 1(a) shows the dimensions of a plate-fin heat sink without a fillet profile. The base dimension is 40 mm x 39.7 mm in size, with a thickness of 5 mm. The channel width and fin thickness are assumed to remain constant over the length of the base and measure 3.3 mm and 1 mm respectively. An optimum fillet radius of 1.5 mm is used for the plate-fin heat sink with fillet profile shown in Figure 1 (b) as discussed in Ref. [20]. The fin heights in Figure 1(a) and (b) were varied by 25 mm and 28.6 mm respectively to remove solid material from the fin base to create fillets that were added to the fin height; hence, making the fin height for plate-fin heat sinks with fillet profile greater [20, 21]. In contrast to the previous study e.g. [20,21], the removed material from the fin base is attached to the plate-fins using half-round pins in the proposed designs as detailed in Ref. [31]. Table 1 provides the geometries dimension and arrangement in details.

**Table 1:** Dimensions of various plate-fin heat sink (HFPS 1 to HFPS 4) designs

Geometry Parameters	PFHS 1	PFHS 2	PFHS 3	PFHS 4
Length, L (mm)	39.7	39.7	39.7	39.7
Width, W (mm)	40.0	40.0	40.0	40.0
Height, H (mm)	25.0	28.6	25.0	25.0
Base Thickness, B (mm)	5.0	5.0	5.0	5.0
Number of Fins	10	10	10	10
Fin Thickness, F (mm)	1.0	1.27	1.27	1.27
Width Channel (mm)	3.3	3.0	3.0	3.0
Fillet Radius, R (mm)	-	1.5	1.5	1.5
Number of Half-Round Pin	-	-	108	108
Half-Round Pin Radius, HR (mm)	-	-	0.635	0.635

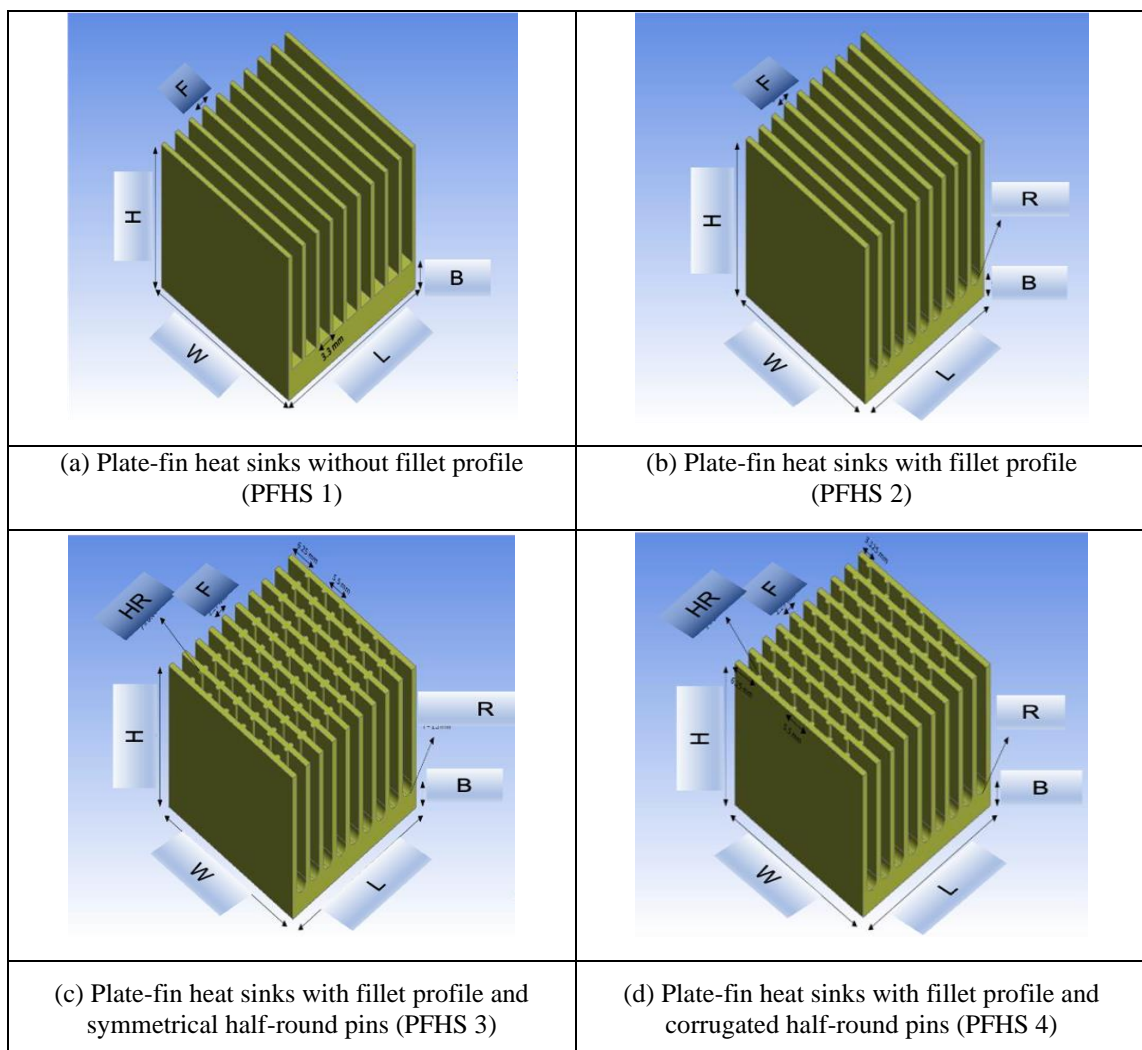


**Figure 1.** Geometrical model of plate-fin heat sinks

As shown in Figure 1(a)-(d), four geometries including plate-fin heat sinks without fillet profile, plate-fin heat sinks with fillet profile, and new proposed designs of plate-fin heat sinks with fillet profile attached with symmetrical half-round pins in and corrugated half-round pins are investigated in this research. Both designs with attached half-round pins are arranged in vertical arrangement as shown in Figure 2. For the remainder of this paper, the plate-fin heat sink subjected to impinging flow is defined as air impinging on the heat sink along the y-axis direction and subsequently flowing parallel to the x-axis. Meanwhile, for the plate-fin heat sink subjected to parallel flow, the air flows into the heat sink across the x-axis direction.

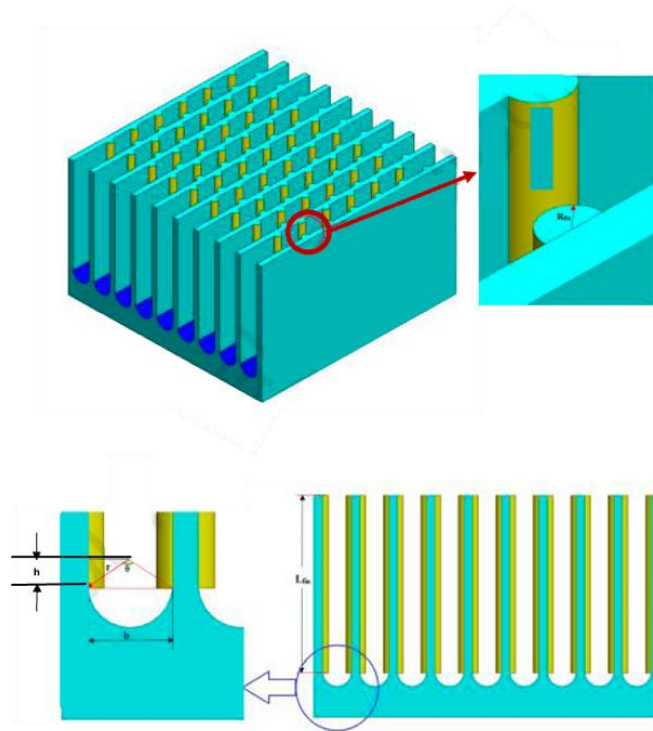


**Figure 2.** Detailed design of fillet profile and half-round pins in PFHS 3 and PFHS 4

### 2.2 Grid generation

ANSYS FLUENT R21 was used to create a computational grid and a three-dimensional discretized model of the plate-fin heat sinks in the pre-processor phase. The complete geometry was discretized into finite volume hexahedral grids as in Ref. [21]. ANSYS FLUENT R21 was used to create a computational grid and a three-dimensional discretized model of the plate-fin heat sinks in the pre-processor phase.

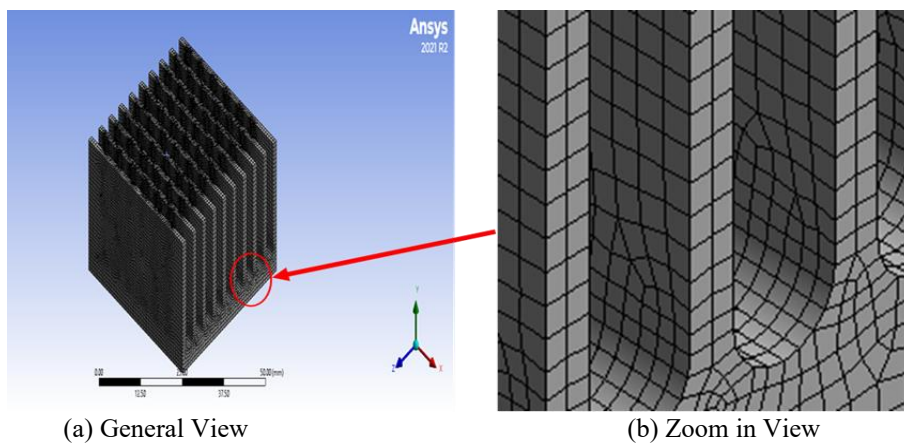


**Figure 3.** Meshing configuration

In addition, as the number of grid elements has a substantial influence on the numerical simulation outcome, mesh independency tests were done for different grid element numbers.

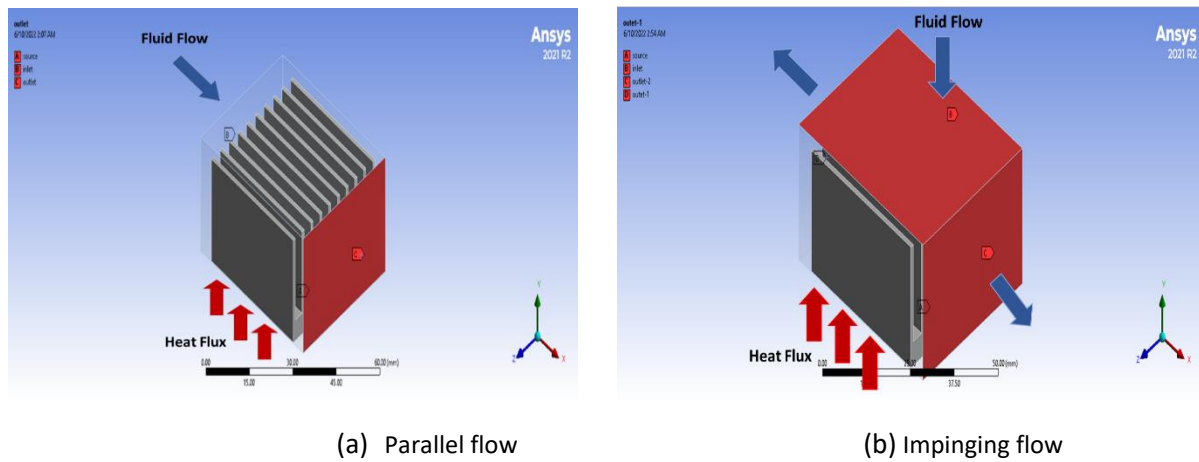
**Table 2: Grid Independence Test**

Plate-Fin Heat Sink	No of Element ( $10^6$ )	Base Temperature (K)	Temperature Difference
PFHS 1	0.79	390.24	-
	1.51	390.22	0.02
	2.82	389.94	0.28
PFHS 2	2.26	385.39	-
	5.77	385.52	0.13
	9.56	385.86	0.34
PFHS 3	2.08	369.25	-
	2.96	369.65	0.40
	3.64	369.76	0.11
PFHS 4	2.83	362.13	-
	3.10	362.85	0.72
	4.63	363.27	0.42

Table 2 shows the numerical results for the base temperature with different mesh configurations. It is clear that an increase in the number of grid elements does not result in significant changes to the base temperature. Mesh with fewer grid components was used to speed up processing. The semi-implicit method for pressure linked equation (SIMPLE) algorithm was used for pressure-velocity coupling applications.

**2.3 Boundary Conditions**

In the solver execution phase of the development of CFD analysis, boundary conditions are considered similar to the experiment work published by Kim et al. [9]. The plate-fin heat sink was made of aluminum alloy 6061. A constant heat flux of  $18750 \text{ W/m}^2$  was provided by an electrical heater to warm up a plate-fin heat sink subjected to impinging flow with variable values of inlet air flow i.e., (0.00092, 0.00218, 0.0033 and 0.00433) kg/s as shown in Figure 4. In addition, the inlet air temperature was set to be at 300 K.



**Figure 4.** Numerical analysis of computational domain with boundary conditions

**2.4 Governing Equations and Numerical Modeling**

The governing equations for conservation of momentum, conservation of mass, and assuming the conjugate heat transfer i.e., Navier-Stokes, continuity, and energy equations are solved numerically to get the convective heat transfer characteristics. The bellow assumptions are considered:

1. The fluid flow is steady state, single phase and incompressible.
2. The flow is turbulent.
3. Three-dimension fluid-solid conjugate is considered.
4. All physical properties of coolant air depend on its mean temperature.

The Navier-Stokes equations across x, y and z directions are given as set of Equation (1) [32]:

$$\begin{aligned}\nabla(\rho\vec{U}u) &= -\frac{\partial p}{\partial x} + \frac{\partial\tau_{xx}}{\partial x} + \frac{\partial\tau_{xy}}{\partial y} + \frac{\partial\tau_{zx}}{\partial z} \\ \nabla(\rho\vec{U}v) &= -\frac{\partial p}{\partial y} + \frac{\partial\tau_{xy}}{\partial x} + \frac{\partial\tau_{yy}}{\partial y} + \frac{\partial\tau_{zy}}{\partial z} \\ \nabla(\rho\vec{U}w) &= -\frac{\partial p}{\partial z} + \frac{\partial\tau_{xz}}{\partial x} + \frac{\partial\tau_{yz}}{\partial y} + \frac{\partial\tau_{zz}}{\partial z}\end{aligned}\quad (1)$$

where  $\rho$  is fluid density,  $\vec{U}$  is the fluid velocity with the velocity components (u, v and w) in three directions, P is pressure and  $\tau$  is the viscous stress tensor.

The energy equation is given by Eq. (2) as following [33]:

$$\nabla(\rho h\vec{U}) = -p\nabla\vec{U} + \nabla(k\nabla T) + \phi + s_h \quad (2)$$

where h is the enthalpy, k is thermal conductivity, T is temperature,  $\phi$  is the dissipation term and  $s_h$  is the source term.

The energy equation for the conduction (solid), which occurs through the different materials is given by Eq. (3) as the following [34]:

$$K_m = \left(\frac{\partial^2 T}{\partial x^2} + \frac{\partial^2 T}{\partial y^2} + \frac{\partial^2 T}{\partial z^2}\right) = 0 \quad (3)$$

where  $K_m$  is the thermal conductivity of the material.

Finally, the continuity equation is described by Eq. (4):

$$\nabla(\rho\vec{U}) = 0 \quad (4)$$

Based on the above equations, a separate solution is used. A sequential technique is utilized to solve the momentum and continuity equations. Due to the nonlinearity of the governing equations, the solution loop is iterated numerous times to obtain a convergent solution. The continuity, momentum, and energy equations are solved using the finite volume method, in which the integral version of the governing equations is solved using a continuum approach. The mathematical equations to describe temperature, pressure, and velocity are obtained in this manner. The convergence for momentum, mass and energy imbalance lesser than  $10^6$  is adopted.

## 2.5 Calculation procedure

The average Nusselt number,  $\overline{Nu}$ , is based on the following Eq. (5):

$$\overline{Nu} = \frac{\bar{h}D_h}{K_a} \quad (5)$$

where  $\bar{h}$  is the mean heat transfer coefficient,  $D_h$  is the hydraulic diameter of the inlet and  $K_a$  is the thermal conductivity of fluid (air). The latter is tabulated based on the mean temperature of air,  $T_m$  given by Eq. (6) as follows:

$$T_m = \frac{(T_{avr} + T_b)}{2} \quad (6)$$

where  $T_b$  the temperature of fin base while  $T_{avr}$  represents the average air temperature as defined in Eq. (7):

$$T_{avr} = \frac{(T_{out} + T_{in})_a}{2} \quad (7)$$

where  $T_{out}$  and  $T_{in}$  are outlet and inlet of air temperature respectively. In Eq. (5), the mean heat transfer coefficient,  $\bar{h}$  is given by:

$$\bar{h} = \frac{Q}{A_T(T_b - T_m)} \quad (8)$$

where  $Q$ ,  $A_T$ ,  $T_b$  and  $T_m$  are the heat transfer rate to the air, the total area that is subjected to the air, the temperature of the fin base and the mean temperature of air respectively. In Eq. (8), the heat transfer rate to the air,  $Q$  and total cooling area,  $A_T$  can be expressed by Eq. (9) and Eq. (10) respectively:

$$Q = \dot{m}C_{Pa}(T_{out} + T_{in}) \quad (9)$$

where  $\dot{m}$  is the mass flow rate and  $C_{Pa}$  is the specific heat of air.

$$A_T = WL + 2N_fH[L + t] + 2B[L + W] \quad (10)$$

where  $W$  and  $L$  are width and length of the heat sink respectively,  $N_f$  represents the number of fins,  $H$ ,  $t$  and  $B$  are the height, thickness of fins and height of the base respectively.

The mean heat transfer coefficient,  $\bar{h}$  can be calculated by substituting Eq. (9) and Eq. (10) into Eq. (8):

$$\bar{h} = \frac{\dot{m}C_{Pa}(T_{out} + T_{in})}{(WL + 2N_fH[L + t] + 2B[L + W])(T_b - T_m)} \quad (11)$$

Substituting Eq. (11) into Eq. (5) gives the average Nusselt number as prescribed by Eq. (12).

$$\overline{Nu} = \frac{\dot{m}C_{Pa}(T_{out} + T_{in})D_h}{(WL + 2N_fH[L + t] + 2B[L + W])(T_b - T_m)K_a} \quad (12)$$

The thermal resistance,  $R_{th}$  of plate-fin heat sinks in Eq. (13) is crucial for understanding the results of the CFD analysis reported in this paper.

$$R_{th} = \frac{1}{\bar{h}A_T} \quad (13)$$

### 3.0 RESULTS AND DISCUSSION

#### 3.1 Validation of the study

Experiment work carried out by Kim et. al [9] based on the geometry of plate-fin heat sink without fillet profile and impinging air flow was used as comparison to validate the computational model accuracy. As listed in the methodology, the boundary conditions for the model applied was similar to the experiment work. The validation was made for the thermal resistance at different mass flow rates as presented in Figure 5.

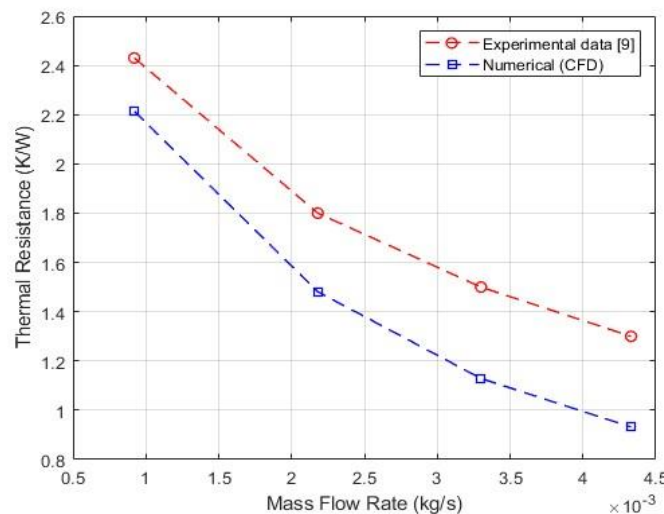


**Figure 5.** Thermal resistance profiles for validation of computational numerical approach at different mass flow rates

The thermal resistance results between the computational numerical approach and the experiment data of Kim et. al [9] are similar in profile but with a maximum deviation of approximately 0.36 K/W, or 27% from the experiment values. The difference might be due to variations in experiment operating conditions such as the applied heat flux and its distribution uniformity, as well as the existence of mixed fluid stream trajectories at high flow rates. Also, the computational setting produced smooth inlet streamlines as compared to the physically chaotic nature of fan-blown air streams. Due to the difficulty to physically control the fluid mechanics of the impinging jet stream, the similarity in the thermal resistance profile of the computational model with a difference of only 20% from the experiment results is deemed acceptable. Hence, the computational model was considered as validated for further case studies.

### 3.2 Comparison of thermal performance of various designs of plate-fins heat sink

This section compares the thermal performance of the proposed designs subjected to both parallel and impinging flow. The comparison made is based on the base temperature, thermal resistance and Nusselt number of the plate-fin heat sink designs.

#### 3.2.1 Parallel flow

A set of examples of the temperature contour for all plate-fin heat sink designs subjected to parallel flow at constant mass flow rate of 0.00092 kg/s are presented in Figure 6. For all cases, the local fin surface temperature was evidently lower at the inlet region due to higher heat transfer mechanics, mainly influenced by the greater bulk temperature difference at the inlet region. As the fluid flow moved parallel to the fins, the local fin surface temperature gradually increased as the bulk temperature difference decreased. This is due to the effects of boundary layer thickness at the leading edge which is thinner compared to at the trailing edge.

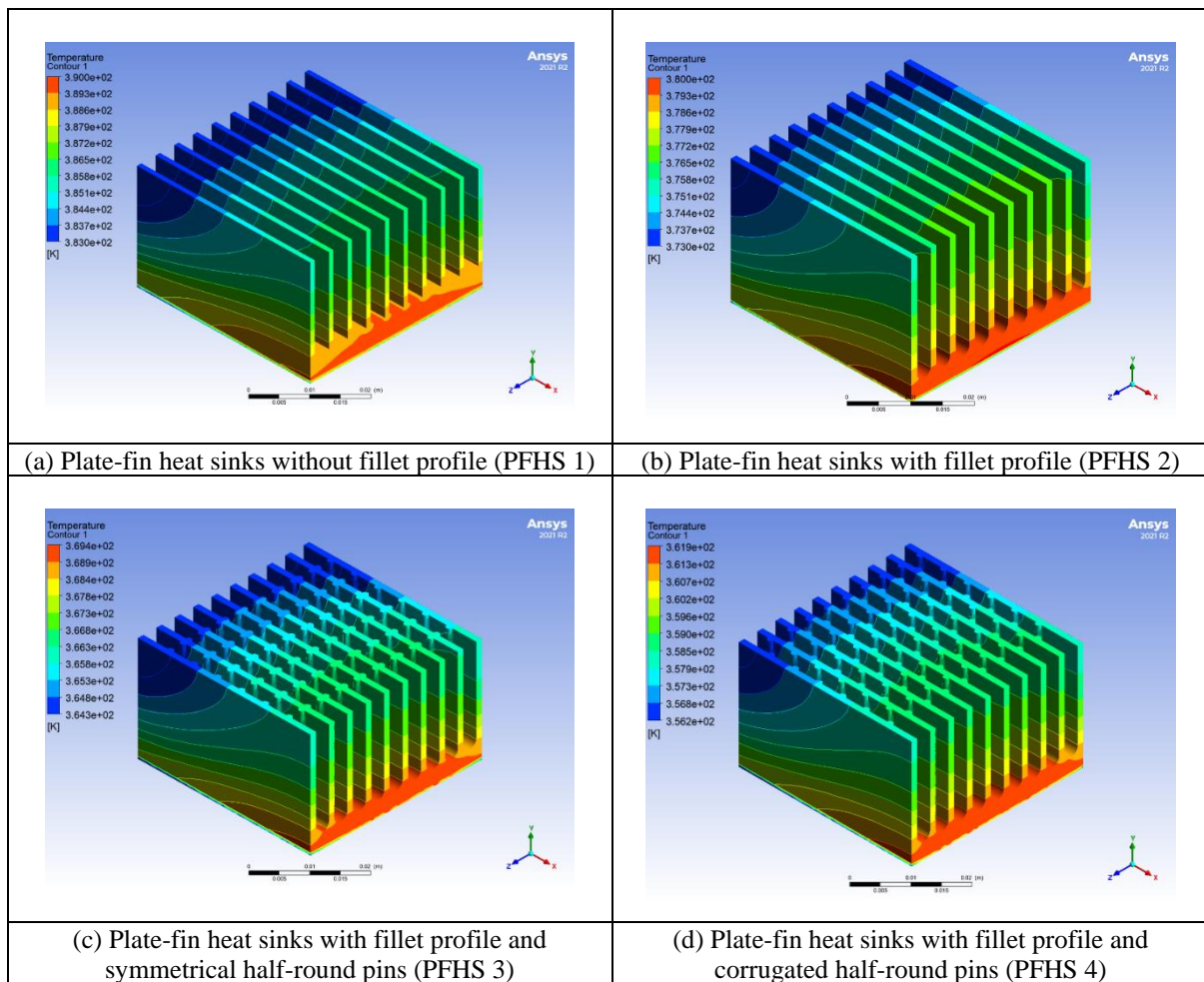


**Figure 6.** Example of temperature contour of the plate-fin heat sinks designs subjected to parallel flow

To investigate the thermal performance of plate-fin heat sinks with different attached half-round pins configuration subjected to parallel flow, the changes in the base temperature, thermal resistance and Nusselt number of different designs are compared at various mass flow rates as shown in Figure 7, 8 and 9 respectively.

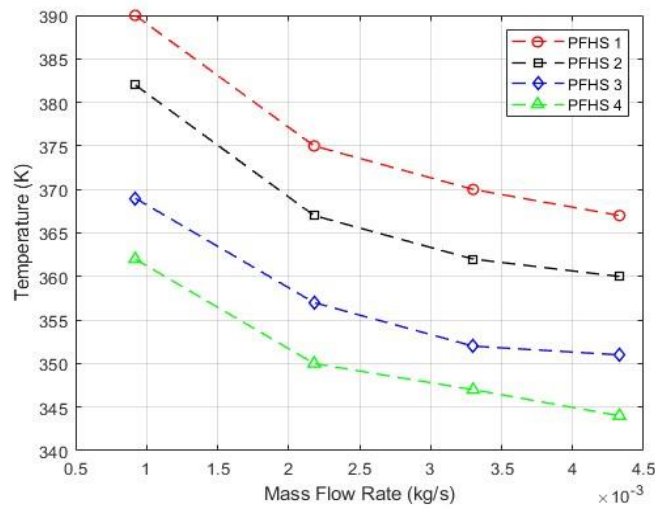


**Figure 7.** The base temperature for different designs subjected to parallel flow at different flow rates

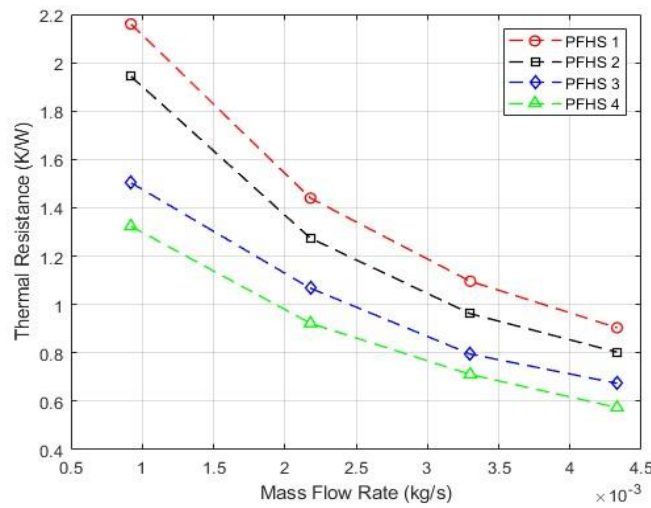


**Figure 8.** The thermal resistance for different designs subjected to parallel flow at different flow rates

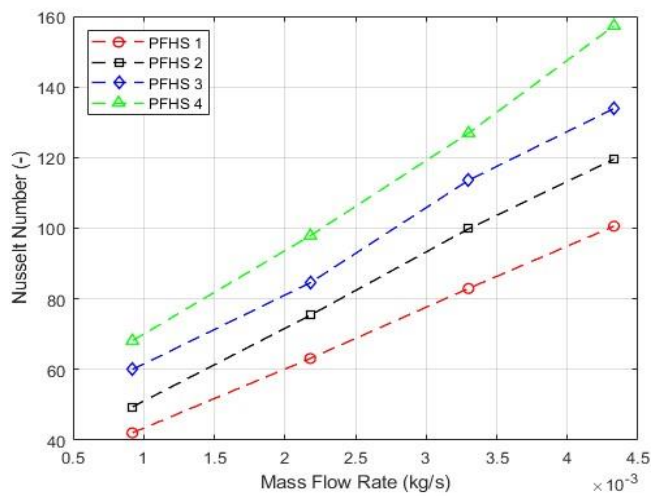


**Figure 9.** Nusselt Number for different designs subjected to parallel flow at different flow rates

Figure 7 compares the base temperatures for all design configurations, and an exponential reduction of the base temperature is seen as the flow rate increases linearly. The existence of fillets at the fin base improves the heat transfer as the base temperature is reduced by approximately 2%. The plate-fin heat sinks with fillet profile and corrugated half-round pins (PFHS 4) show the best thermal performance for parallel flow as it registers the lowest base temperature and the lowest thermal resistance (as shown in Figure 8). From Figure 9, corrugated half-round pins (PFHS 3 and 4) evidently increases the Nusselt number by 40% compared to design PFHS1 and 2 without the corrugated half-round pins. This is mainly attributed to the creation of mixed flows within the thermal region as the fluid streams is diverted intermittently through the pins as it flows along the fin configuration, creating micro zones of turbulence near the fin surfaces.

### 3.2.2 Impinging flow

A sample of the temperature contour of the heat sink designs subjected to impinging flow at constant mass flow rate of 0.00092 kg/s is presented in Figure 10.

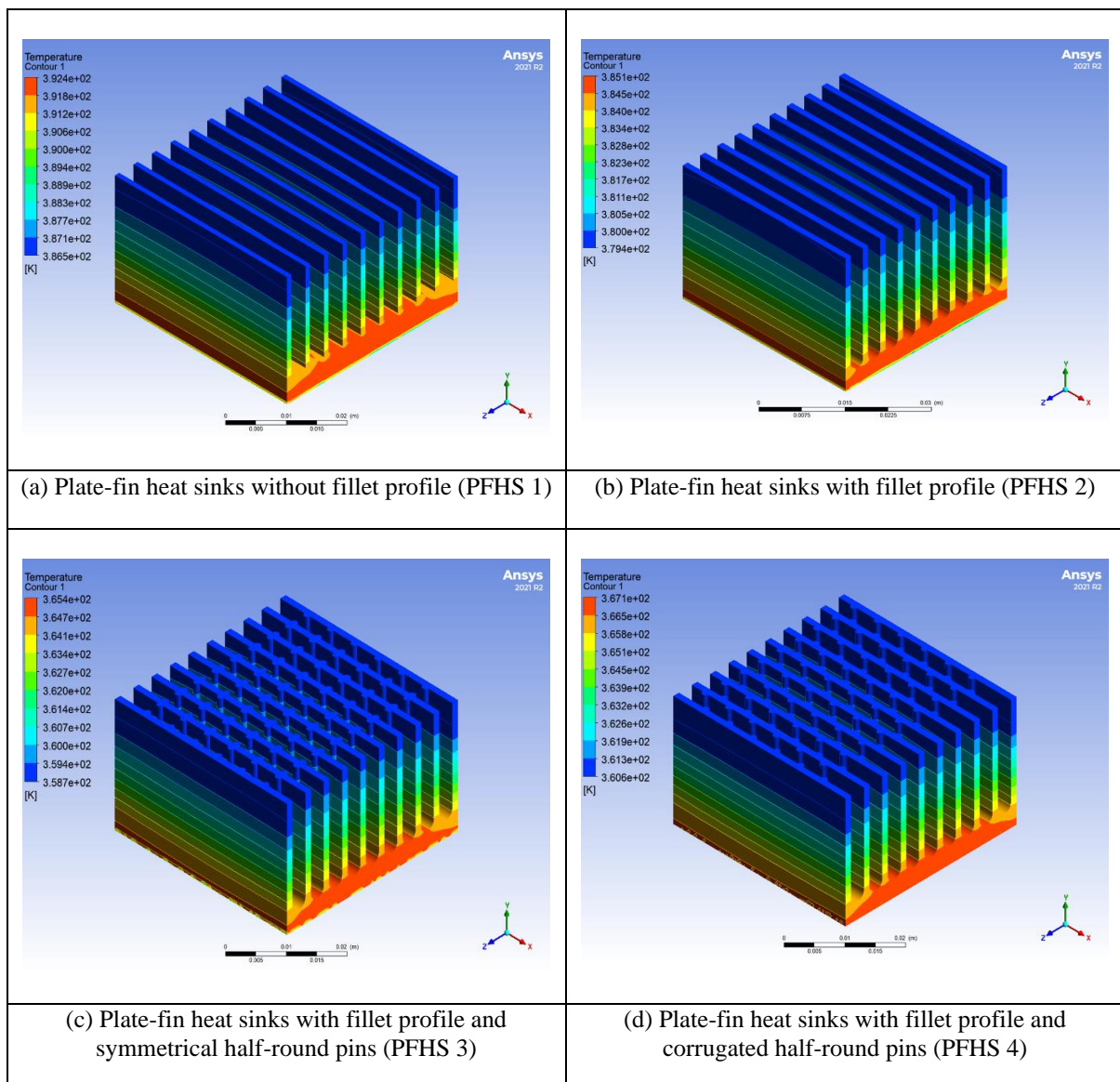


**Figure 10.** Temperature contour of the plate-fin heat sinks with different designs at a fixed mass flow subjected to impinging flow

The result shows that the plate-fin heat sinks with fillet profile and symmetrical half-round pins (PFHS 3) have the lowest base temperature compared to other designs. Apart from this, even though the temperature contours do not show a significant change in different configurations, the maximum temperature measured is meaningfully

different for the studied configurations i.e., 392 K, 385 K, 365 K and 367 K for Figure 10(a)-(d) respectively. Furthermore, the average temperature is lower for the inlet of air flow which is at top region of the heat sink. As the flow moves downward in y-direction, the average temperature increases gradually and shows the highest value at the base of the heat sink. Besides, the temperature contours are less effective in heat distribution when compared to the results presented in Section 3.2.1.

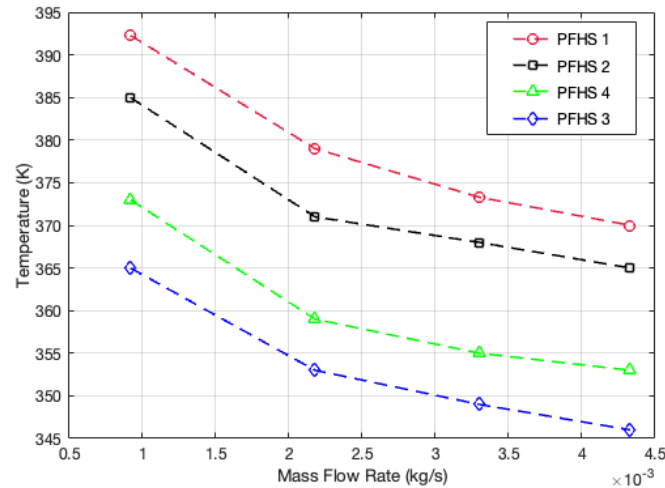


**Figure 11.** Comparison of the base temperature for different designs subjected to impinging flow at different mass flow rates

The results show a slight enhancement in terms of thermal performance when PFHS 3 is subjected to impinging flow. According to Figure 11, plate-fin heat sinks with fillet profile and symmetrical half-round pins (PFHS 3) have the lowest base temperature among other designs when subjected to impinging flow at various mass flow rates. For the remainder of the result, it shows that the temperature decreases when the mass flow rate is increased. Based on this result, the thermal resistance is also expected to be the same pattern as the result presented in Section 3.2.1 where the thermal resistance decreases as the mass flow rate is increased. Meanwhile, the Nusselt number increases when the mass flow rate is increased.

#### 4.0 CONCLUSION

Thermal performance of different design of plate-fin heat sinks with and without fillet profile subjected to parallel and impinging flow has been investigated and compared. The two new proposed designs for plate-fin heat sinks with fillet profile are introduced. The removed material from the fin base to create the fillet is re-used to form half-round pin that is attached to the plate-fin, in symmetrical and corrugated arrangements. The results have shown that the plate-fin heat sink with fillet profile and corrugated half-round pins (PFHS 4) have the best thermal performance among other designs when subjected to parallel flow. The base temperature and thermal resistance are lower while the Nusselt number is higher when compared to plate-fin heat sinks with fillet profile (PFHS 2). Meanwhile, when they are subjected to impinging flow, the plate-fin heat sink with fillet profile and symmetrical half-round pin (PFHS 3) have the best thermal design among other designs. This study has provided a platform for further work, for example, investigating the heat transfer characteristics for both proposed designs experimentally which is useful for validation process of numerical work. Furthermore, studying the thermal performance with different pin shape i.e., square pin or hexagon with various pin parameters may also be included in further work.

#### ACKNOWLEDGEMENT

This research was funded by a grant from Universiti Teknologi MARA, UiTM (MYRA Grant 600-RMC/GPM ST 5/3 (036/2021)).

#### REFERENCES

- [1] Raunt, S. V., and B. S. Kothavale. "Study on thermal performance of micro fin heat sink under natural convection—A Review." *International Journal of Current Engineering and Technology* (2017): 257-261.
- [2] Jadhav, Mahesh, Rahul Awari, Diksha Bibe, Amol Bramhane, and Mayura Mokashi. "Review on enhancement of heat transfer by active method." *International Journal of Current Engineering and Technology* 6 (2016): 221-225.

- [3] Sonawane, Tejas, Prafulla Patil, Abhay Chavhan, and B. M. Dusane. "A review on heat transfer enhancement by passive methods." *International Research Journal of Engineering and Technology* 3, no. 9 (2016): 1567-1574.
- [4] Bar-Cohen, Avram. "Thermal management of electronic components with dielectric liquids." *JSME International Journal Series B Fluids and Thermal Engineering* 36, no. 1 (1993): 1-25. <https://doi.org/10.1299/jsmeb.36.1>
- [5] Forghan, Fariborz, Donald Goldthwaite, Matthew Ulinski, and Hameed Metghalchi. "Experimental and theoretical investigation of thermal performance of heat sinks." In *annual meeting for ISME, United States, May*. 2001.
- [6] Kordyban, Tony, and Anthony J. Rafanelli. "Hot air rises and heat sinks: Everything you know about cooling electronics is wrong." (1998): 395-395. <https://doi.org/10.1115/1.2792653>
- [7] Kondo, Yoshihiro, and Hitoshi Matsushima. "Study of impingement cooling of heat sinks for LSI packages with longitudinal fins." *Heat Transfer-Japanese Research: Co-sponsored by the Society of Chemical Engineers of Japan and the Heat Transfer Division of ASME* 25, no. 8 (1996): 537-553. [https://doi.org/10.1002/\(sici\)1520-6556\(1996\)25:8<537::aid-hjt4>3.0.co;2-y](https://doi.org/10.1002/(sici)1520-6556(1996)25:8<537::aid-hjt4>3.0.co;2-y)
- [8] Li, Hung-Yi, Shung-Ming Chao, and Go-Long Tsai. "Thermal performance measurement of heat sinks with confined impinging jet by infrared thermography." *International Journal of Heat and Mass Transfer* 48, no. 25-26 (2005): 5386-5394.
- [9] Kim, Dong-Kwon, Sung Jin Kim, and Jin-Kwon Bae. "Comparison of thermal performances of plate-fin and pin-fin heat sinks subject to an impinging flow." *International Journal of Heat and Mass Transfer* 52, no. 15-16 (2009): 3510-3517. <https://doi.org/10.1109/ijtherm.2008.4544292>
- [10] Hosseinirad, E., M. Khoshvaght-Aliabadi, and F. Hormozi. "Effects of splitter shape on thermal-hydraulic characteristics of plate-pin-fin heat sink (PPFHS)." *International Journal of Heat and Mass Transfer* 143 (2019): 118586. <https://doi.org/10.1016/j.ijheatmasstransfer.2019.118586>
- [11] Lin, Sheam-Chyun, Fu-Sheng Chuang, and Chien-An Chou. "Experimental study of the heat sink assembly with oblique straight fins." *Experimental Thermal and Fluid Science* 29, no. 5 (2005): 591-600. DOI: [10.1016/j.expthermflusci.2004.08.003](https://doi.org/10.1016/j.expthermflusci.2004.08.003)
- [12] Huang, Guei-Jang, Shwin-Chung Wong, and Chun-Pei Lin. "Enhancement of natural convection heat transfer from horizontal rectangular fin arrays with perforations in fin base." *International Journal of Thermal Sciences* 84 (2014): 164-174. <https://doi.org/10.1016/j.ijthermalsci.2014.05.017>
- [13] Abdullah, H. AlEsa, M. Maqableh Ayman, and Ammourah Shatha. "Enhancement of natural convection heat transfer from a fin by rectangular perforations with aspect ratio of two." *International Journal of physical sciences* 4, no. 10 (2009): 540-547.
- [14] Dhanawade, Kavita H., Vivek K. Sunnapwar, and Hanamant S. Dhanawade. "Thermal analysis of square and circular perforated fin arrays by forced convection." *International Journal of Current Engineering and Technology* 2 (2014): 109-114. <https://doi.org/10.14741/ijcet/spl.2.2014.20>
- [15] Huang, Ren-Tsung, Wen-Junn Sheu, and Chi-Chuan Wang. "Orientation effect on natural convective performance of square pin fin heat sinks." *International Journal of Heat and Mass Transfer* 51, no. 9-10 (2008): 2368-2376. <https://doi.org/10.1016/j.ijheatmasstransfer.2007.08.014>
- [16] AlEsa, Abdullah HM. "Augmentation of fin natural convection heat dissipation by square perforations." *Journal of Mechanical Engineering and Automation* 2, no. 2 (2012): 1-5. <https://doi.org/10.5923/j.jmea.20120202.01>
- [17] Liu, Minghou, Dong Liu, Sheng Xu, and Yiliang Chen. "Experimental study on liquid flow and heat transfer in micro square pin fin heat sink." *International Journal of Heat and Mass Transfer* 54, no. 25-26 (2011): 5602-5611. <https://doi.org/10.1016/j.ijheatmasstransfer.2011.07.013>
- [18] AlEsa, Abdullah H., and Mohamad I. Al-Widyan. "Enhancement of natural convection heat transfer from a fin by triangular perforation of bases parallel and toward its tip." *Applied Mathematics and Mechanics* 29, no. 8 (2008): 1033-1044. <https://doi.org/10.1007/s10483-008-0807-x>
- [19] Freegah, Basim, Ammar A. Hussain, Abeer H. Falih, and Hossein Towsyfyhan. "CFD analysis of heat transfer enhancement in plate-fin heat sinks with fillet profile: Investigation of new designs." *Thermal Science and Engineering Progress* 17 (2020): 100458. <https://doi.org/10.1016/j.tsep.2019.100458>
- [20] Wong, Kok-Cheong, and Sanjiv Indran. "Impingement heat transfer of a plate fin heat sink with fillet profile." *International Journal of Heat and Mass Transfer* 65 (2013): 1-9. <https://doi.org/10.1016/j.ijheatmasstransfer.2013.05.059>
- [21] Hussain, Ammar A., Basim Freegah, Basima Salman Khalaf, and Hossein Towsyfyhan. "Numerical investigation of heat transfer enhancement in plate-fin heat sinks: Effect of flow direction and fillet profile." *Case Studies in Thermal Engineering* 13 (2019): 100388. <https://doi.org/10.1016/j.csite.2018.100388>
- [22] Elnaggar, Mohamed HA. "Heat transfer enhancement by heat sink fin arrangement in electronic cooling." *Heat Transfer* 2, no. 3 (2015).

- [23] Li, Hung-Yi, Kuan-Ying Chen, and Ming-Hung Chiang. "Thermal-fluid characteristics of plate-fin heat sinks cooled by impingement jet." *Energy Conversion and Management* 50, no. 11 (2009): 2738-2746. <https://doi.org/10.1016/j.enconman.2009.06.030>
- [24] Li, Hung-Yi, Ming-Hung Chiang, Chih-I. Lee, and Wen-Jei Yang. "Thermal performance of plate-fin vapor chamber heat sinks." *International Communications in Heat and Mass Transfer* 37, no. 7 (2010): 731-738. <https://doi.org/10.1016/j.icheatmasstransfer.2010.05.015>
- [25] Teertstra, P., M. M. Yovanovich, and J. R. Culham. "Analytical forced convection modeling of plate fin heat sinks." *Journal of Electronics Manufacturing* 10, no. 04 (2000): 253-261. <https://doi.org/10.1142/s0960313100000320>
- [26] Khan, Waqar A., J. Richard Culham, and M. Michael Yovanovich. "Optimization of pin-fin heat sinks using entropy generation minimization." *IEEE Transactions on Components and Packaging Technologies* 28, no. 2 (2005): 247-254. <https://doi.org/10.1109/tcapt.2005.848507>
- [27] Copeland, David. "Optimization of parallel plate heatsinks for forced convection." In *Sixteenth Annual IEEE Semiconductor Thermal Measurement and Management Symposium (Cat. No. 00CH37068)*, pp. 266-272. IEEE, 2000. <https://doi.org/10.1109/stherm.2000.837093>
- [28] Biber, Catharina R. "Pressure drop and heat transfer in an isothermal channel with impinging flow." *IEEE Transactions on Components, Packaging, and Manufacturing Technology: Part A* 20, no. 4 (1997): 458-462. DOI: [10.1109/STHERM.1997.566800](https://doi.org/10.1109/STHERM.1997.566800)
- [29] Saini, Manish, and Ralph L. Webb. "Validation of models for air cooled plane fin heat sinks used in computer cooling." In *ITherm 2002. Eighth Intersociety Conference on Thermal and Thermomechanical Phenomena in Electronic Systems (Cat. No. 02CH37258)*, pp. 243-250. IEEE, 2002. <https://doi.org/10.1109/itherm.2002.1012464>
- [30] Duan, Zhipeng, and Y. S. Muzychka. "Pressure drop of impingement air cooled plate fin heat sinks." (2007): 190-194. <https://doi.org/10.1115/1.2721094>
- [31] B. Freegah, A.A. Hussain, A.H. Falih, H. Towsyfyhan. "CFD analysis of heat transfer enhancement in plate-fin heat sinks with fillet profile: investigation of new designs", *Thermal Science and Engineering Progress* (2019): <https://doi.org/10.1016/j.tsep.2019.100458>
- [32] Young, Donald F., Bruce R. Munson, Theodore H. Okiishi, and Wade W. Huebsch. *A brief introduction to fluid mechanics*. John Wiley & Sons, 2010.
- [33] Hoffmann, Klaus A., and Steve T. Chiang. "Computational fluid dynamics volume I." *Engineering education system* (2000).
- [34] Blazek, Jiri. *Computational fluid dynamics: principles and applications*. Butterworth-Heinemann, 2015.